molecular pharmaceutics

ARTICLE

pubs.acs.org/molecularpharmaceutics

Biological Evaluation of a Novel Doxorubicin−Peptide Conjugate for Targeted Delivery to EGF Receptor-Overexpressing Tumor Cells

Shibin Ai,*,† Jianli Duan,† Xin Liu,† Stephanie Bock,† Yuan Tian,‡ and Zebo Huang*,†,§

†College of Pharmacy, Wuhan University, Wuhan 430071, China

‡Union Hospital, Tongji Medical College, Huazhong University of Science and Technology, Wuhan 430021, China

§Research Center of Food and Drug Evaluation, Wuhan University, Wuhan 430071, China

ABSTRACT: Epidermal growth factor receptor (EGFR) is overexpressed in a variety of epithelial malignancies and thus can be used for EGFR-targeted therapy to improve antitumor efficacy. Therefore we synthesized a novel conjugate of doxorubicin (DOX) with an EGFR-binding peptide (NH_2-CMYIEALDKYAC-COOH; EBP) via an ester bond at position 14 of DOX through a glutarate spacer. To confirm that the DOX−EBP conjugate is capable of targeting tumor cells overexpressing EGFR, we compared the cellular accumulation, intracellular distribution and *in vitro* cytotoxicity of DOX−EBP and free DOX. After treating with equimolar concentration of DOX−EBP or free DOX, the conjugate accumulated at significantly higher levels in EGFR-overexpressing cells than in non-EGFR-overexpressing cells, while the intracellular accumulation of free DOX was almost the same in all the cells. However, the intracellular accumulation of DOX−EBP was significantly reduced in EGFR-overexpressing cells preincubated with inhibitory anti-EGFR monoclonal antibody, demonstrating the involvement of EGFR pathway in the transport of the conjugate. Confocal fluorescence microscopy reveals that the conjugate was distributed in cytoplasmic and perinuclear areas during the first 30 min, whereas the free DOX was accumulated in both cytoplasm and nuclei. After 24 h, however, the DOX signal in the cells treated with DOX−EBP was also distributed in the nuclei, suggesting the release of DOX from the conjugate and entry into the nuclei. Biodistribution and *in vivo* antitumor experiments, together with *in vitro* cytotoxicity, indicate that the therapeutic competence of DOX−EBP was due to its increased accumulation in EGFR-expressing tumor cells. Furthermore, the survival of tumor-bearing mice treated with DOX−EBP was significantly higher than that with free DOX. These data demonstrate the enhanced anticancer efficacy and reduced systemic toxicity of DOX−EBP conjugate with targeting ability to EGFR-overexpressing tumor cells.

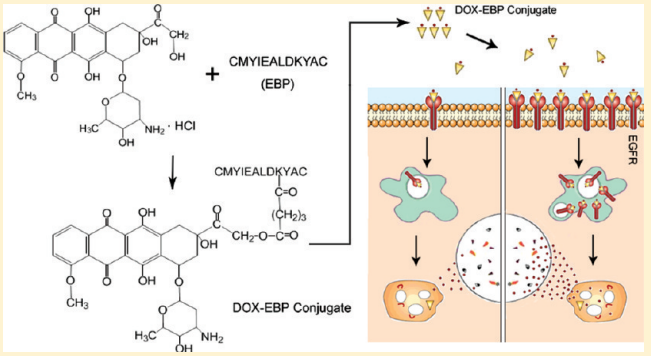

KEYWORDS: epidermal growth factor receptor, peptide, doxorubicin, drug delivery

INTRODUCTION

Doxorubicin (DOX), an anthracycline antibiotic, has been widely used in chemotherapy for treatment of leukemia, colon cancer, breast cancer and many other types of cancer, and has become one of the most commonly used anticancer drugs.[1,2] The mechanism of DOX to kill tumor cells has mainly been related to its intercalation into DNA and disruption of topoisomerase II activity.[3] However, due to its lack of specific targeting to tumor cells, DOX has shown a large-spread field of systemic toxicities in healthy tissues.[4,5] In particular, the extensive use of DOX in the clinical setting may cause serious irreversible cardiac toxicity.[6,7]

In order to enhance the anticancer efficacy and to reduce the systemic toxicity of DOX, a number of studies have used overexpressed receptors on the surface of tumor cells as DOX target sites and accordingly designed drug molecules or delivery systems to distribute DOX to tumor cells.[8−10] The strategy involves the conjugation of DOX with a target-specific vector, which disposes of a high cellular binding affinity to the targeted site.[11,12] For example, DOX was conjugated to a cyclic pentapeptide (CNGRC) via a hydrolyzable spacer to target CD13 on the surface of the SK-UT-1 cells, and the DOX-CNGRC conjugate was reported to alter the cellular uptake process of DOX.[13] AN-152, a conjugate of DOX covalently linked with the luteinizing hormone-releasing hormone (LHRH), was reported to bind specifically to LHRH receptors and act as a chemotherapeutic agent after internalization of the ligand−receptor complex into cancer cells expressing LHRH,[9] and a phase II clinical study of the conjugate was started in 2008.[14]

Epidermal growth factor receptor (EGFR) is an important transmembrane receptor comprising an extracellular ligand-binding

Received: July 27, 2010
Accepted: January 17, 2011
Revised: January 10, 2011
Published: January 17, 2011

domain, a transmembrane domain and an intracellular domain with tyrosine kinase activity.[15] Since EGFR is overexpressed or abnormally activated in a number of malignancies and highly related to proliferation, angiogenesis, invasion and metastasis of tumor cells,[16] it has been increasingly used as a potential target for cancer therapeutics. Several EGFR targeting agents have been developed as anticancer drugs, including (1) monoclonal antibodies such as cetuximab and panitumumab, which target the extracellular domain of the receptor and inhibit the ligand-dependent EGFR signal transduction, and (2) small-molecule inhibitors such as gefitinib and erlotinib, which target the intracellular tyrosine kinase domain of EGFR.[17,18]

Epidermal growth factor (EGF) is one of the most important EGFR ligands with high binding ability and selectivity.[19] The structure of EGF molecule contains 3 loops which are held in place by 3 disulfide bonds:[20,21] loop A, Cys^6 and Cys^{20}; loop B, Cys^{14} and Cys^{31}; and loop C, Cys^{33} and Cys^{42}. The B-loop is implicated in EGFR binding,[22−24] and the active region is CMYIEALDKYAC,[25] which may be used as a vector to conjugate DOX to specifically target tumor cells expressing EGFR.

In this study, we synthesized the EGFR-binding peptide (EBP: NH_2-CMYIEALDKYAC-COOH) and conjugated it with DOX via an ester bond at position 14 through a glutarate spacer. To confirm the EGFR-targeted chemotherapy of DOX−EBP conjugate, we tested the intracellular accumulation levels of the conjugate in tumor cells with different EGFR expression levels and investigated the cellular entry pathway of DOX−EBP conjugate by blocking EGFR function using an anti-EGFR monoclonal antibody. We also compared the cytotoxicity of the conjugate and free DOX in tumor cells *in vitro* as well as their distribution and antitumor effect *in vivo*.

MATERIALS AND METHODS

Chemicals and Reagents. Doxorubicin hydrochloride (DOX HCl) salt, daunorubicin hydrochloride (internal standard), glutaric anhydride, piperidine and 1-hydroxybenzotriazole were from Sigma-Aldrich (St. Louis, MO, USA). Trifluoroacetic acid (TFA) was obtained from Rhodia (France). *N*-(9-Fluorenylmethoxycarbonyloxy) succinimide (Fmoc-OSu), benzotriazol-1-yloxytris(dimethylamino)phosphonium hexafluorophosphate (BOP), *N*,*N*-dimethylformamide (DMF) and *N*,*N*-diisopropylethylamine (DIPEA) were purchased from GL Biochem (Shanghai, China).

Tumor Cell Lines. Human colon cancer cell line SW480, human gastric cancer cell line SGC-7901, human breast cancer cell line MCF-7, and murine melanoma cell line B16 were obtained from China Center for Type Culture Collection (CCTCC, Wuhan, China). The cells were cultured in RPMI-1640 medium (Gibco BRL, GrandIsland, NY) containing 10% fetal bovine serum (Hyclone, Logan, UT), 10^5 U/L penicillin and 100 mg/L streptomycin at 37 °C.

Synthesis of DOX−Peptide Conjugate. The Fmoc protected EBP (Fmoc-NH-CMYIEALDKYAC-COOH) was synthesized via solid phase methodology using Rink Amide methylbenzhydrylamine (MBHA) resin and Fmoc strategy. The synthesized peptide was purified using reversed phase high performance liquid chromatography (RP-HPLC) on a preparative C_{18} column after TFA cleavage.[26] The DOX−peptide conjugate was synthesized essentially as described by Nagy et al. (1996) using EBP as the peptide.[27] Briefly, to a solution of DOX HCl in DMF, Fmoc-OSu and DIPEA were added, and the reaction mixture was stirred at room temperature for 3 h. The resulting *N*-Fmoc-DOX crystals were collected by filtration and washed with cold diethyl ether, and then placed with glutaric anhydride to a round-bottomed flask containing DMF and DIPEA. The mixture was stirred at room temperature for 10 h. After removal of the solvent, the residue was taken up by dichloromethane and washed with water and brine. The obtained *N*-Fmoc-DOX-14-*O*-hemiglutarate was dissolved in Fmoc-NH-CMYIEALDKYAC-COOH solution in DMF. BOP reagent, 1-hydroxybenzotriazole and DIPEA were then added and stirred for 1 h. The solvent was removed, and the residual oil was treated with ethyl acetate. The resulting solid was dissolved in DMF, and piperidine was added to remove the protecting groups. The DOX−peptide product was purified by RP-HPLC on a C_{18} column and lyophilized.[28] Purity of the product was determined by HPLC analysis as described below. The product was confirmed by electrospray mass spectra.

HPLC Analysis. DOX content in samples was analyzed using an Agilent 1100 series HPLC systems (Agilent Technologies, Santa Clara, CA) and a Shimadzu RF-10A XL fluorescence detector (Shimadzu Inc., Kyoto, Japan). The analytical column was ODS-C_{18} (5 μm particle size, 250 × 4.6 mm, Thermo Scientific, USA). The mobile phase consisting of a mixture of acetonitrile, methanol and water (32:50:18, v/v/v) was delivered at a flow rate of 1.0 mL/min. The column temperature was maintained at 40 °C. Fluorescence detection was performed using excitation and emission wavelengths of 480 and 580 nm, respectively.

Western Blot Analysis. The expression of EGFR in the tumor cell lines was analyzed by Western blotting.[29] The cells were grown to near confluence in 25 cm^2 culture flasks at a density of 1×10^7 cells/flask. Confluent cells were washed with ice-cold phosphate-buffered saline (PBS), and then treated with lysis buffer containing 50 mM Tris-HCl (pH 7.4), 120 mM NaCl, 1 mM EDTA, 1% TritonX-100 and 1% (v/v) protease inhibitor cocktail (Sigma-Aldrich). The samples were homogenized on ice for 2 min with a Dounce homogenizer, and cellular debris was removed by centrifugation (3000 rpm; 10 min) at 4 °C. The lysates were further centrifuged at 12,000 rpm for 1 h at 4 °C, and the supernatants were stored at −70 °C until use. The protein concentration was quantitated using the Bio-Rad Detergent Compatible Protein Assay kit (Bio-Rad, Hercules, CA). An equal amount of proteins (20 μg per lane) for each sample was separated by SDS−PAGE (12%) and transferred to polyvinylidene difluoride (PVDF) membranes (Millipore, Bedford, MA). The membranes were blocked overnight (4 °C) in Tris-buffered saline containing 0.05% (v/v) Tween-20 (TBS-T) and 5% (m/v) nonfat dried milk, and were incubated with anti-EGFR antibody (Santa Cruz Biotechnology, Inc., Santa Cruz, CA) or anti-β-actin antibody (Sigma-Aldrich). After removal of the primary antibody, the membranes were washed with TBS-T and incubated for 1 h at room temperature with a secondary horseradish peroxidase-coupled IgG antibody (Pierce Chemical, Rockford, IL). The membranes were washed for 3 times with TBS-T. Specific protein bands were visualized using enhanced chemoluminescence (ECL) according to the protocol of the manufacturer (Amersham Biosciences Inc., Piscataway, NJ).

Determination of Cellular DOX Content. Intracellular accumulation levels of DOX and DOX conjugate in different EGFR expressing cells were determined by HPLC analysis.[30] SW480, SGC-7901, B16 and MCF-7 cells were grown in 25 cm^2 culture flasks with normal medium to ~80% confluence (1×10^7 cells/flask).

After careful removal of medium, the cells were incubated with 5 mL of fresh serum-free medium containing 0.5 μM free DOX or DOX−EBP conjugate at 37 °C for indicated times. The cells were then washed 3 times with ice-cold PBS to remove unbound DOX or DOX−peptide conjugate, collected by centrifugation, and counted using a Coulter counter, and daunorubicin was added as an internal standard for DOX quantification. The cell pellet was then thoroughly extracted with an equal volume of chloroform and isopropanol mixture (3:1, v/v) and centrifuged at 13,000 rpm for 2 min. The drug levels in the cell lysates were quantified by HPLC analysis as described above. The DOX concentration was given by the standard curve, and the cellular drug content was shown as pg of DOX/cell.

EGFR Inhibition Assay. To test the cellular entry pathway of DOX−EBP conjugate, SW480, SGC-7901, B16 and MCF-7 cells were preincubated with 5 mL of fresh serum-free medium containing 5 μg/mL anti-EGFR monoclonal antibody C225 (ImClone Systems, Inc., New York, NY) for 12 h at 37 °C.[31] After removal of the pretreatment solution, the cells were washed once with PBS solution and further incubated with 5 mL of fresh serum-free medium containing 0.5 μM free DOX or DOX−EBP conjugate at 37 °C for indicated times. Cellular DOX content was measured by HPLC as described above, and the C225 prompted reduction of cellular DOX accumulation was used as an inhibition index of cellular DOX uptake.

Laser Scanning Confocal Fluorescence Microscopy. Since DOX and DOX conjugate are autofluorescent at an excitation wavelength of 488 nm, the detection of DOX and the conjugate was performed using a laser scanning confocal fluorescence microscope (Fluoview FV300, Olympus, Japan) at λ_{ex} = 480 nm and λ_{em} = 580 nm.[13,14] In order to investigate the intracellular distribution of fluorescent DOX and DOX conjugate in different EGFR expressing cells, SW480 and MCF-7 cells were seeded on glass coverslips in 24-well plates (5×10^4 cells per well). After 24 h, the cells were washed with serum-free medium, treated with 0.5 μM free DOX or DOX−EBP conjugate (prepared in RPMI-1640 serum-free medium prior to use) and incubated at 37 °C for indicated times. At the end of the treatment, the cells were examined under laser confocal fluorescence microscope. To detect nuclei, the cells were stained with 1 μg/mL of 4′,6-diamidino-2-phenylindole (DAPI) (Sigma-Aldrich) at room temperature for 10 min and visualized by fluorescence microscopy at λ_{ex} = 350 nm and λ_{em} = 460 nm.[32,33] To further characterize the selective cellular uptake of DOX−EBP conjugate via EGFR-mediated pathway, the cells were preincubated with C225 for 12 h at 37 °C. Following the removal of the pretreatment solution, the cells were washed with serum-free medium, treated with free DOX or DOX−EBP conjugate and incubated at 37 °C for indicated times. The cells were visualized using the laser scanning confocal fluorescence microscope, and the fluorescent intensity of cells was analyzed using Image-Pro Plus 6.0 for Windows (Media Cybernetics, Silver Spring, MD).

***In Vitro* Cytotoxicity Assay.** The cytotoxicity of free DOX and DOX−EBP conjugate was evaluated using a modified MTT cell viability assay.[34,35] SW480, SGC-7901, B16 and MCF-7 cells were seeded in 96-well plates at a density of 5×10^3 cells/well and grown in normal medium for 24 h. The medium was then replaced with serum-free medium containing a series of concentration of DOX or DOX−EBP conjugate, and the cells were further incubated at 37 °C for 5 or 48 h as indicated; the cells incubated in serum-free medium without any drug were used as blank controls. After adding 20 μL of 5 mg/mL MTT solution in PBS to each well, the plates were further incubated for 4 h. The cells were then solubilized in 100 μL of DMSO solution. The absorbance was read at 570 nm (test wavelength) and 630 nm (reference wavelength) on a microplate reader (Bio-Rad Model 450, Hercules, CA, USA).

Tumor Xenograft Model. Inbred C57BL/6 (H-2^b) mice (18 to 22 g; 6−8 weeks old) of both sexes were used for B16 xenograft model.[36] Mice were obtained from the Experimental Animal Center of Tongji Medical College, Huazhong University of Science and Technology (Wuhan, China), and all experimental procedures involving animals were approved by the Animal Care and Use Committee of Huazhong University of Science and Technology. Male and female mice were housed separately in polycarbonate cages, and provided with food and water *ad libitum*. Tumors were grown at the lateral flank by sc injection of 1×10^7 murine melanoma B16 cells and randomized to constitute groups for distribution assay and antitumor activity assay *in vivo*.[37,38]

Evaluation of Drug Distribution in Tumor-Bearing Mice. To evaluate the distribution of DOX−EBP conjugate *in vivo*, the C57BL/6 mice were used for the B16 xenograft model. The model mice were randomly divided into groups, which contained 48 animals each. Control mice were given injections of 100 μL of PBS. The experimental mice received equimolar amounts of free DOX or DOX−EBP conjugate (6 mg/kg DOX or equivalent), which were injected once into the tail vein at 2 weeks after tumor implantation with an average tumor size of 450 to 550 mm^3. At selected time points (0.25, 0.5, 1, 2, 4, 8, 24, and 48 h) after injection, blood was collected from the mice and centrifuged to separate the plasma. The plasma was divided into 2×50 μL aliquots and immediately frozen at −80 °C. The mice were then sacrificed by cervical dislocation, and the liver, lungs, kidneys, heart and tumor tissues were excised, washed with sterilized saline solution, and cut into small pieces in 2 mL of PBS. The tissues were homogenized in Ultra-Turrax T18 Homogenizer (IKA, USA). All tissues were labeled and placed into polypropylene cryovials and immediately frozen at −80 °C until analysis. Plasma and tissues from nondosed mice (n = 24) were also collected for the preparation of standard curves. The DOX content in plasma and tissues was determined by HPLC analysis as described above.[38,39]

Evaluation of Antitumor Activity of DOX−EBP Conjugate. To test the *in vivo* efficacy of DOX−EBP conjugate, one day after transplantation of tumors, animals bearing B16 xenografts were randomly divided into groups. Each group contained nine animals. The experimental mice were injected once with free DOX (5 mg/kg) or DOX−EBP conjugate (5 mg/kg DOX equivalent) into the tail vein at days 1, 8, and 15 after transplantation of tumors; the control mice received injections of saline. Tumors were measured twice weekly by vernier calipers, and the tumor volume was calculated using the following formula: volume (mm^3) = (length) × $(\text{width})^2/2$.[40] Animal survival was monitored daily, and survival data were presented in a Kaplan−Meier plot.[41]

Statistical Analysis. Data were presented as mean ± SD and evaluated by Student's t-test using SPSS 13.0 for Windows (SPSS Inc., Chicago).

RESULTS

Synthesis of DOX−EBP Conjugate. The EGFR-binding peptide was selected as a vector in the present study and

Scheme 1. Synthesis of DOX−EBP Conjugate from Doxorubicin Hydrocholoride[a]

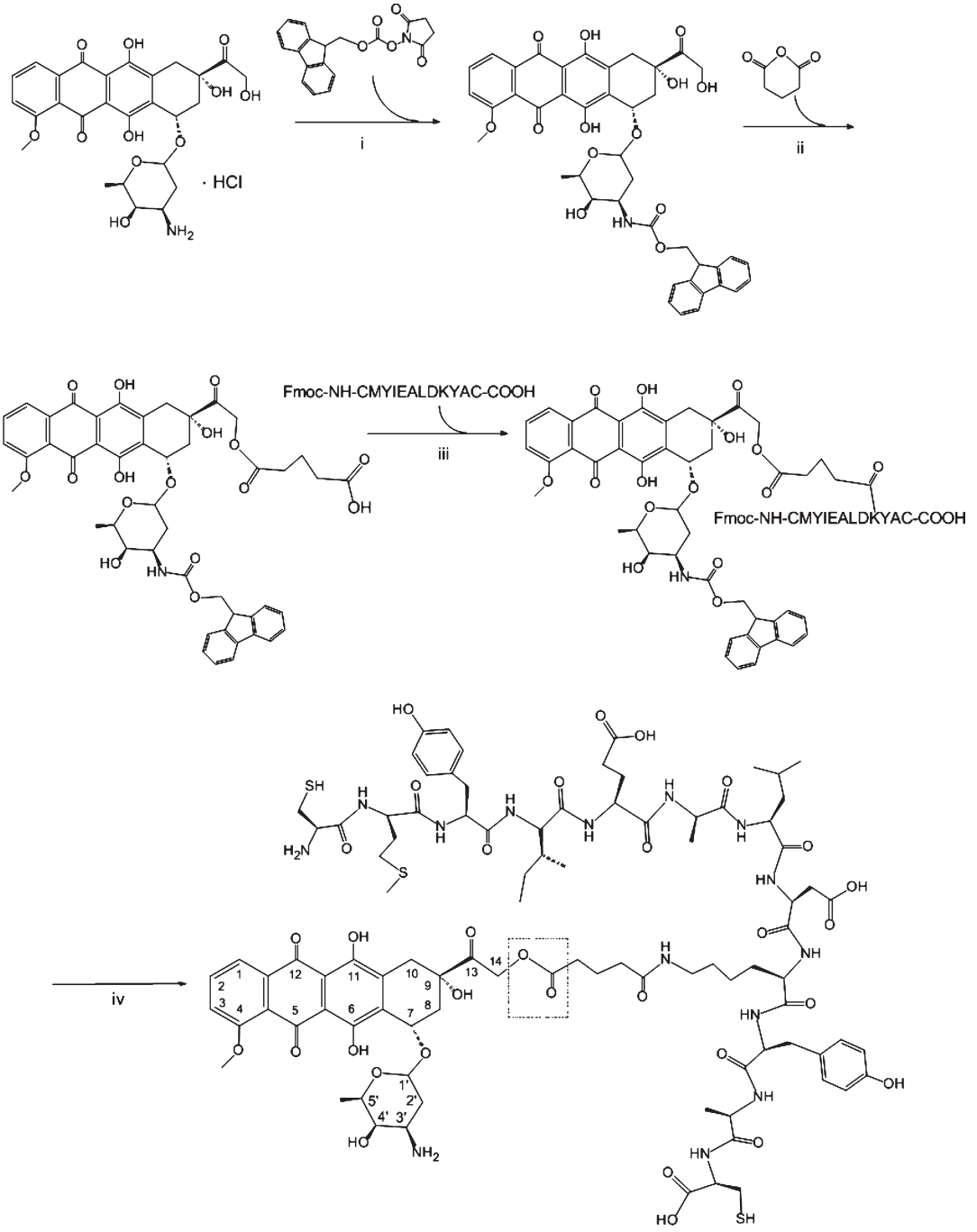

[a] Reagents: (i) *N*,*N*-dimethylformamide (DMF), *N*-(9-fluorenylmethoxycarbonyloxy) succinimide (Fmoc-OSu), *N*,*N*-diisopropylethylamine (DIPEA), trifluoroacetic acid (TFA), and then diethyl ether; (ii) glutaric anhydride, DMF, DIPEA, and then TFA; (iii) Fmoc-NH-CMYIEALDKYAC-COOH, DMF, DIPEA, benzotriazol-1-yloxytris(dimethylamino)phosphonium hexafluorophosphate (BOP), and then ethyl acetate; (iv) DMF and piperidine; TFA, pyridine and DMF; and then ethyl acetate. The ester bond between the 14-OH group of DOX and glutaric acid is indicated by a dashed line frame.

synthesized using a solid phase methodology.[26] DOX was conjugated via an ester bond at its C_{14} with EBP through a glutarate spacer.[27] As shown in Scheme 1, *N*-(9-fluorenylmethoxycarbonyl)-DOX (*N*-Fmoc-DOX) was prepared by linking *N*-(9-fluorenylmethoxycarbonyloxy) succinimide (Fmoc-OSu) with DOX at the 3′ amino group. *N*-Fmoc-DOX-14-*O*-hemiglutarate was obtained using glutaric anhydride,[28] identified by RP-HPLC and further confirmed by MS and NMR. The *N*-Fmoc-DOX-14-*O*-hemiglutarate was then conjugated with Fmoc-NH-CMYIEALDKYAC-COOH through D-Lys,[9] and the Fmoc group was removed with piperidine. The DOX−peptide product was purified by RP-HPLC on a C_{18} column and lyophilized.[29] The purity of the product was determined by analytical HPLC, and the percentage of surface area was used to

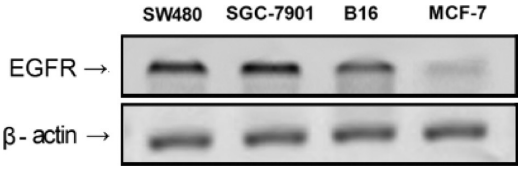

Figure 1. EGFR expression in SW480, SGC-7901, B16 and MCF-7 cells. Cell lysates were prepared from SW480 (lane 1), SGC-7901 (lane 2), B16 (lane 3) and MCF-7 (lane 4) cells, separated by SDS−PAGE, and analyzed by Western blotting.

Table 1. The Intracellular Levels of DOX in Selected Cell Lines after 1 and 12 h of Incubation with Free DOX or DOX−EBP Conjugate[a]

	intracellular DOX levels (pg/cell)			
	1 h		12 h	
cells	free DOX	DOX−EBP	free DOX	DOX−EBP
SW480	0.51 ± 0.08	0.19 ± 0.04	0.62 ± 0.07	0.80 ± 0.05
SGC-7901	0.57 ± 0.05	0.21 ± 0.06	0.63 ± 0.05	0.93 ± 0.06
B16	0.50 ± 0.08	0.16 ± 0.05	0.65 ± 0.07	0.78 ± 0.05
MCF-7	0.65 ± 0.24	0.05 ± 0.03	0.50 ± 0.06	0.17 ± 0.04

[a] Cells were grown in 25 cm^2 culture flasks with normal medium to ~80% confluence (1×10^7 cells/flask). After careful removal of medium, 5 mL of serum-free medium containing 0.5 μM of free DOX or DOX−EBP conjugate was added, and the cells were further incubated at 37 °C for indicated times. The DOX content in the cell lysates was quantified by HPLC. Values are presented as the mean ± SD (n = 6).

assess the purity (95%). The DOX−EBP product was confirmed by electrospray mass spectra (direct injection): m/z (ESI), 1944 $[M + H]^+$. The yield from DOX HCl to the final product was 40%.

Expression of EGFR in Tumor Cells. The baseline EGFR expression levels of the four tumor cell lines SW480, SGC-7901, B16 and MCF-7 were confirmed by Western blot analysis. While MCF-7 was non-EGFR-overexpressing cells, the other three were EGFR-overexpressing cell lines (Figure 1). These results are in agreement with previous reports.[42−45]

Accumulation of DOX−EBP Conjugate in Tumor Cells with EGFR Overexpression. To test whether DOX−EBP conjugate can be selectively delivered into the tumors that overexpress EGFR, the cellular DOX levels in different EGFR expressing cells treated with the conjugate were compared with that treated with free DOX. After incubation with free DOX or DOX−EBP conjugate, the cellular DOX contents were determined by HPLC. No difference in intracellular DOX levels was observed in all the tested cell lines after incubation with free DOX for 1 h, whereas the DOX levels in EGFR-overexpressing cells (SW480, SGC-7901 and B16) were significantly higher than those in non-EGFR-overexpressing cells (MCF-7) when treated with DOX−EBP conjugate for 1 h (Table 1). Similar results were also observed after 12 h of incubation with free DOX or the conjugate (Table 1). These data demonstrate a distinct cellular entry of DOX−EBP conjugate from that of the free DOX.

Entry of DOX−EBP Conjugate into Tumor Cells through EGFR-Mediated Pathway. Anti-EGFR monoclonal antibody C225 can block the binding sites of EGFR to its ligands[15,31,46] and thus can be used to inhibit cellular entry of drugs through

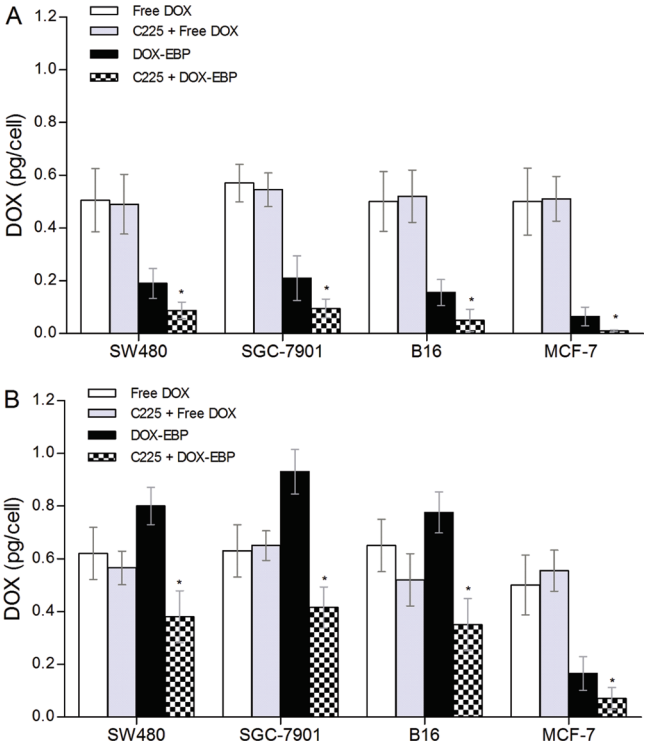

Figure 2. Intracellular accumulation of free DOX and DOX−EBP conjugate in tumor cells. SW480, SGC-7901, B16 and MCF-7 cells were treated with free DOX or DOX−EBP for 1 h (A) and 12 h (B). The intracellular DOX levels were determined by HPLC and expressed as pg of DOX/cell. Data represent mean ± SD of 6 samples for each cell line. *p < 0.05 (with versus without C225 pretreatment).

EGFR-mediated pathway. Therefore, to investigate whether the cellular uptake of DOX−EBP conjugate was mediated by EGFR, an EGFR inhibition assay was conducted through competitive blockade of EGFR with C225. The cells were preincubated with C225 for 12 h and then treated with free DOX or DOX−EBP. After 1 h of incubation with free DOX, no significant difference of cellular DOX level was observed in all tested cell lines with or without C225 preincubation (Figure 2A). However, after 1 h of incubation with DOX−EBP conjugate, the intracellular DOX accumulation was reduced in all the cells preincubated with C225 as compared to those of corresponding cells without C225 pretreatment (Figure 2A). Similar trend was also found for the 12 h treatment with free DOX or DOX−EBP after C225 preincubation (Figure 2B), demonstrating the effectiveness of C225 to inhibit cellular uptake of DOX−EBP and thus the involvement of EGFR in the cellular delivery of the conjugate.

Cellular Uptake and Intracellular Localization of DOX−EBP Conjugate. To further compare the cellular uptake pathways of free DOX and DOX−EBP conjugate, EGFR-overexpressing SW480 cells and non-EGFR-overexpressing MCF-7 cells were incubated with free DOX or the conjugate and evaluated by confocal fluorescence microscopy. As shown in Figure 3A, DOX was present in nuclei as well as in cytoplasmic region of both SW480 and MCF-7 cells after 30 min of incubation with free DOX, as revealed by superimposition of red fluorescence from DOX and blue fluorescence from DAPI. The DOX fluorescence intensity was also the same in both SW480 and MCF-7 cells as assessed by Image-Pro Plus software (Figure 3A). After the cells were incubated with DOX−EBP

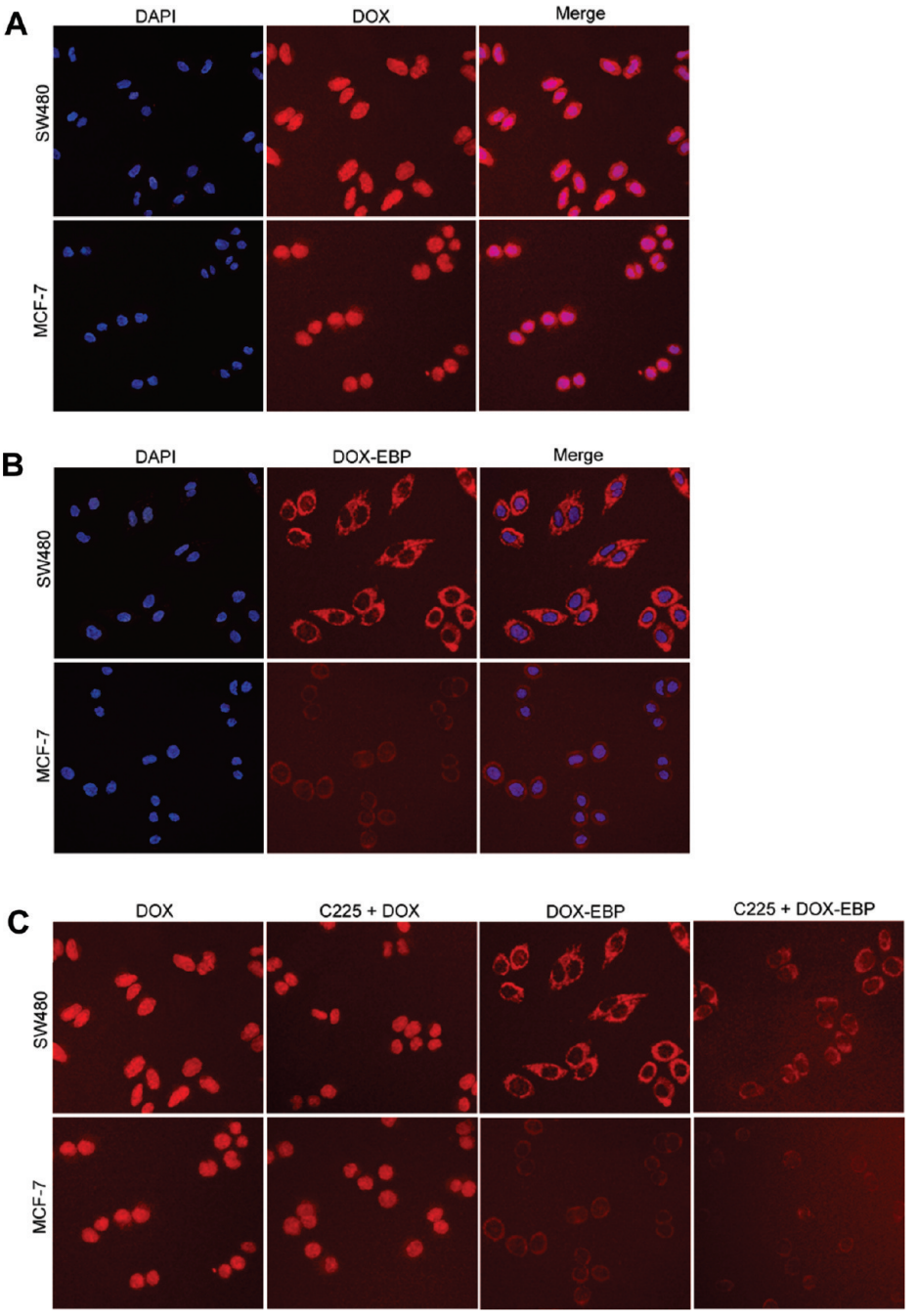

Figure 3. Intracellular distribution of free DOX and DOX−EBP conjugate in SW480 and MCF-7 cells after 30 min of drug exposure. The cells were treated with equimolar free DOX (A) or DOX−EBP conjugate (B) for 30 min and visualized under confocal microscope. Merged images display the overlay of nuclear DAPI staining (blue) and DOX autofluorescence (red). Purple represents DOX in nuclear region. To detect the effect of anti-EGFR antibody C225, the cells were preincubated with or without C225 for 12 h and then treated with equimolar free DOX or DOX−EBP for 30 min prior to visualization (C).

conjugate for 30 min, however, DOX was clearly present in cytoplasm and perinuclear region of both cell lines, but the DOX fluorescence intensity in EGFR-overexpressing SW480 cells was much stronger than that in non-EGFR-overexpressing MCF-7 cells (Figure 3B). On the other hand, although preincubation of the cells with anti-EGFR monoclonal antibody C225 had no effect on the intracellular distribution of free DOX, the fluorescence originated from DOX−EBP conjugate was inhibited by the preincubation (Figure 3C). Together, these results further suggest that the small, hydrophobic DOX entered the cytoplasm in a passive manner and rapidly diffused into the nucleus (within 30 min), whereas the DOX conjugate was only visible in cytoplasmic and perinuclear areas, but not in the nucleus, during the first 30 min, indicating a distinct entry pathway of the conjugate from the free DOX.

After 24 h of incubation with free DOX, the intracellular distribution of DOX signal was almost the same as that of 30 min in both SW480 and MCF-7 cells (Figure 4A). However, after the same period of incubation with DOX−EBP conjugate, a stronger DOX fluorescence in both cytoplasm and nuclei was detected in

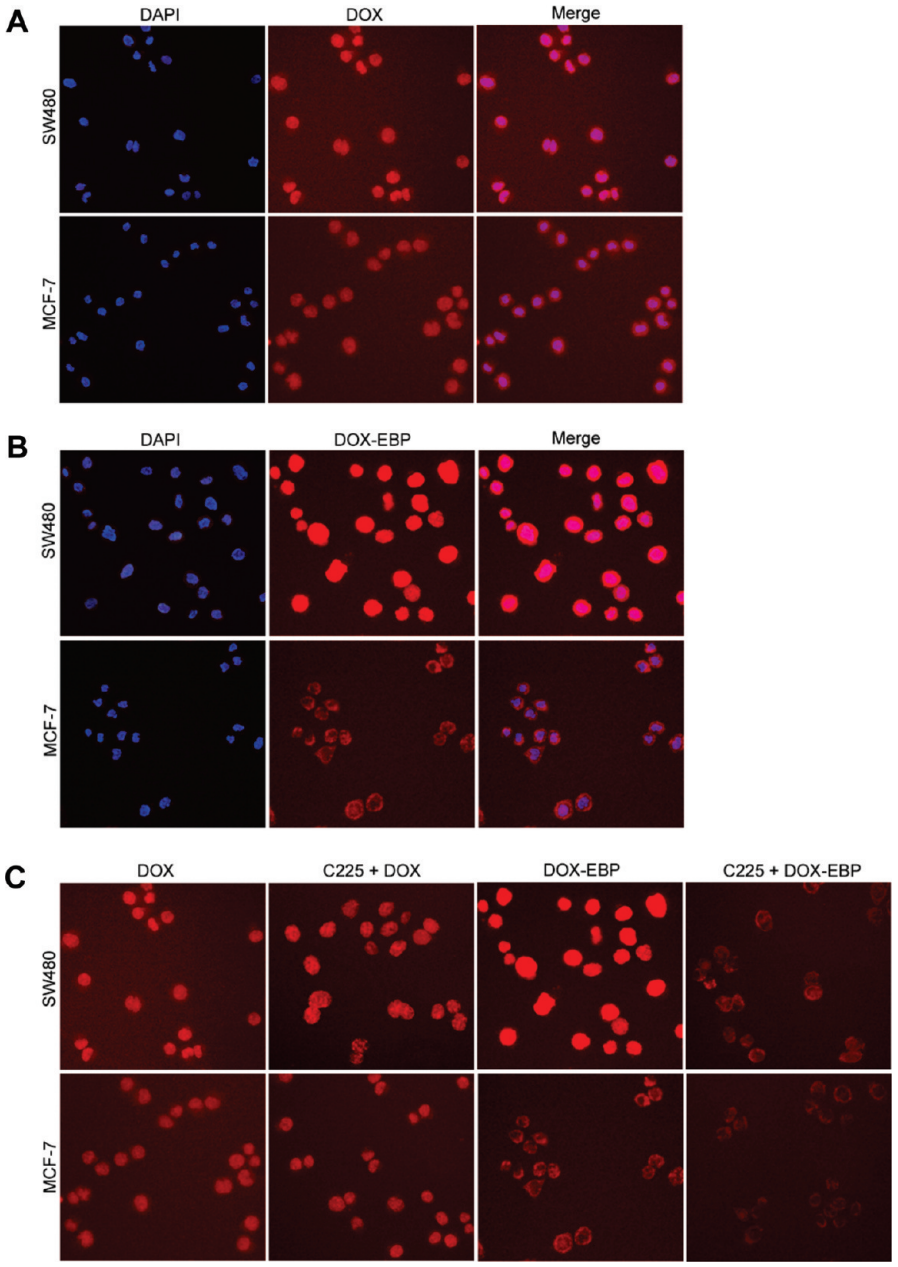

Figure 4. Intracellular distribution of free DOX and DOX−EBP conjugate in SW480 and MCF-7 cells after 24 h of drug exposure. The cells were treated with equimolar free DOX (A) or DOX−EBP conjugate (B) for 24 h and visualized under confocal microscope. Merged images display the overlay of nuclear DAPI staining (blue) and DOX autofluorescence (red). Purple represents DOX in nuclear region. To detect the effect of anti-EGFR antibody C225, the cells were preincubated with or without C225 for 12 h and then treated with equimolar free DOX or DOX−EBP for 24 h prior to visualization (C).

SW480 cells, but only a weak DOX signal in the cytoplasm and an even weaker signal in the nuclei were visible in MCF-7 cells (Figure 4B), which was different from that of the first 30 min treatment with the conjugate (Figure 3B). Preincubation with C225 had no effect on the fluorescence distribution of free DOX in both cell lines, but showed an inhibitory effect on the fluorescence intensity when treated with DOX−EBP conjugate (Figure 4C). These data clearly demonstrate the buildup of DOX fluorescence in the nuclei after prolonged incubation with the conjugate (24 h), and also suggest EGFR-mediated uptake of DOX−EBP conjugate.

***In Vitro* Cytotoxicity of DOX−EBP Conjugate.** In order to compare the cytotoxic effects of DOX−EBP conjugate with free DOX, we selected the four cell lines based on EGFR expression levels as shown in Figure 1. The cells were incubated with a series of concentrations of free DOX or DOX conjugate, and the cell viability was evaluated using the MTT method. As shown in Table 2, the IC_{50} values of DOX−EBP conjugate were much higher than those of free DOX for all tested cell lines after incubation for 5 h, i.e. the cytotoxicity of the conjugate was lower than that of free DOX. However, after 48 h of incubation, the cytotoxicity of the conjugate was much higher than that of free DOX in all the EGFR-overexpressing cell lines (SW480, SGC-7901 and B16) although free DOX was still more cytotoxic than DOX−EBP conjugate in the non-EGFR-overexpressing MCF-7

Table 2. Cytotoxicity of Free DOX and DOX−EBP Conjugate on Tumor Cells[a]

	IC_{50} (μM) of DOX equivalent			
	5 h		48 h	
cells	free DOX	DOX−EBP	free DOX	DOX−EBP
SW480	12.45 ± 1.62	64.37 ± 2.68	0.56 ± 0.16	0.08 ± 0.03
SGC-7901	18.50 ± 2.18	82.16 ± 3.24	0.38 ± 0.10	0.05 ± 0.08
B16	15.58 ± 1.42	76.50 ± 4.74	0.72 ± 0.19	0.16 ± 0.09
MCF-7	17.75 ± 2.38	165.68 ± 3.22	0.45 ± 0.20	6.25 ± 0.65

[a] Cells were seeded in 96-well plates at a density of 5×10^3 cells/well and incubated for 24 h, and then exposed to free DOX or DOX−EBP for 5 and 48 h. Cell viability was assessed by the MTT assay. Data are expressed as mean IC_{50} ± SD (n = 3).

cells (Table 2). These results clearly show that the DOX−EBP conjugate was much more potent than the free DOX after 48 h treatment in EGFR-overexpressing cells.

***In Vivo* Distribution of DOX−EBP Conjugate.** Following a single iv injection of free DOX or DOX−EBP, samples from blood, liver, lung, kidney, heart and tumor tissues of C57BL/6 mice bearing B16 cells were taken and DOX level was measured by HPLC. As shown in Figure 5A, the free DOX rapidly disappeared from the circulation, whereas the DOX−EBP conjugate maintained at high level for a much longer time (up to 48 h). During the drug circulation, the highest level of DOX content in plasma was 22.94 ± 1.68 μg/mL at 0.25 h after injection of DOX−EBP conjugate, whereas that of free DOX was 6.52 ± 0.13 μg/mL (n = 6, mean ± standard deviation).

As the primary site of DOX metabolism, the liver contained the highest level of DOX among all the organs tested. The DOX content in liver reached the highest level (26.03 ± 1.84 μg/g tissue) after the mice were treated with free DOX for 30 min, while the peak appeared at 8 h after administration of DOX−EBP conjugate (Figure 5B). The highest value of DOX content in liver of mice treated with free DOX was 4 times higher than that treated with DOX−EBP conjugate (Figure 5B). Similarly, the DOX levels in lung, kidney and heart of mice treated with free DOX were much higher than those treated with DOX−EBP conjugate (Figure 5C−E).

When DOX−EBP conjugate was injected, the DOX content in tumor tissues was increased with time during the first 8 h and peaked at 25.46 ± 2.19 μg/g tissue, and decreased to 6.68 ± 2.52 μg/g tissue at 48 h (Figure 5F). For free DOX treatment, however, the DOX content rapidly peaked at 8.69 ± 2.17 μg/g tissue within 30 min, and decreased to 1.23 ± 0.75 μg/g tissue at 48 h (Figure 5F). The area under the DOX concentration−time curve (AUC), which is a key therapeutic index of a drug, was calculated (Kinetic software version 4.4.1, Thermo Electron Corp., Waltram, MA) for tumor tissues. As shown in Figure 5F, the $AUC_{0\rightarrow48}$ in tumor tissues after DOX−EBP treatment (861.8 μg h/g) was much higher than that of free DOX (149.6 μg h/g), indicating that DOX concentration in the tumor tissues was significantly higher after administering animals with DOX−EBP than with free DOX.

***In Vivo* Antitumor Therapeutic Efficacy.** Since EGFR is commonly expressed at high levels in a variety of solid tumors,[46,47] it can be used as a target to improve the antitumor effect of drugs and decrease their systemic cytotoxicity. Therefore we tested whether the DOX−EBP conjugate was able to enhance the therapeutic efficacy of DOX against EGFR-expressing tumors and to improve the survival rate of the animals bearing tumor xenograft. As shown in Figure 6A, the reduction of tumor volume in C57BL/6 mice bearing B16 cells was apparent in both free DOX and DOX conjugate groups: at the end of the experiment on day 28, the mean volume of the tumors in the mice treated with free DOX (1585 ± 102 mm^3) and DOX−EBP conjugate (668 ± 180 mm^3) was significantly smaller than that in the control group (1990 ± 222 mm^3), i.e. about 20% and 66% reduction respectively. These data demonstrate that the DOX−EBP conjugate was more efficacious than free DOX in the inhibition of tumor growth.

Due to the lack of selectivity, the systemic cytotoxic chemotherapy of free DOX would result in adverse toxicity. Indeed, although free DOX did inhibit tumor growth compared to the saline control (Figure 6A), the survival of mice bearing tumor xenograft did not significantly improve (Figure 6B): the average survival time was 34 ± 3 days for free DOX treatment and 32.5 ± 2.5 days for the control. On the other hand, however, DOX−EBP conjugate significantly increased the survival time of animals (39.5 ± 3.5 days) under the same conditions (Figure 6B), demonstrating the targeting effect of the DOX−EBP conjugate in chemotherapy.

DISCUSSION

In order to increase the therapeutic efficacy of doxorubicin (DOX) while decreasing its systemic toxicity, a strategy was chosen to enhance tumor specificity of DOX by conjugation to EGFR-binding peptide (EBP), which may help deliver DOX directly to EGFR-overexpressing neoplastic cells. This study investigated the ability of the DOX−EBP conjugate to bind to EGFR-overexpressing cells as well as its antitumor efficacy *in vitro* and *in vivo*.

For targeted delivery, a drug can be linked to a peptide carrier via covalent, ionic or hydrophobic bond, which may result in alteration of structure and activity of the drug. A range of peptides conjugated to DOX through different sites and linkers have been studied. For example, DOX has been conjugated to Vectocell peptides through ester, thioether and amide chemical linkers at position 14 and 3′ amino group of DOX, and the conjugation via chemically stable bonds either at position 14 (thioether) or at position 3′ (amide) of DOX resulted in significant or complete loss of activity while the conjugate via ester bond at C_{14} position increased antitumor efficacy compared to free DOX.[48] Another example is the conjugation of DOX to LHRH via DOX-14-*O*-hemiglutarate, which has fully preserved the binding affinity of the peptide carrier and the cytotoxic activity of DOX.[49] We have shown in this study that the conjugation of DOX via the 14-OH group to EBP has increased both *in vitro* and *in vivo* antitumor activity (Table 2 and Figure 6).

To efficiently target EGFR-overexpressing tumor cells, the DOX−EBP conjugate must preserve the binding ability of EGF to EGFR. As shown in Table 1, the accumulation of free DOX in both EGFR-overexpressing and non-EGFR-overexpressing cells, as determined by HPLC, was almost the same; in contrast, the accumulation of the DOX−EBP conjugate in EGFR-overexpressing cells (SW480, SGC-7901 and B16) was much higher than that in non-EGFR-overexpressing cells. Fluorescent microscopy further demonstrates the high affinity of DOX−EBP conjugate in EGFR-overexpressing cells: the fluorescent intensity in SW480 cells was much higher than that in MCF-7 cells after incubation with DOX−EBP conjugate (Figure 3B and

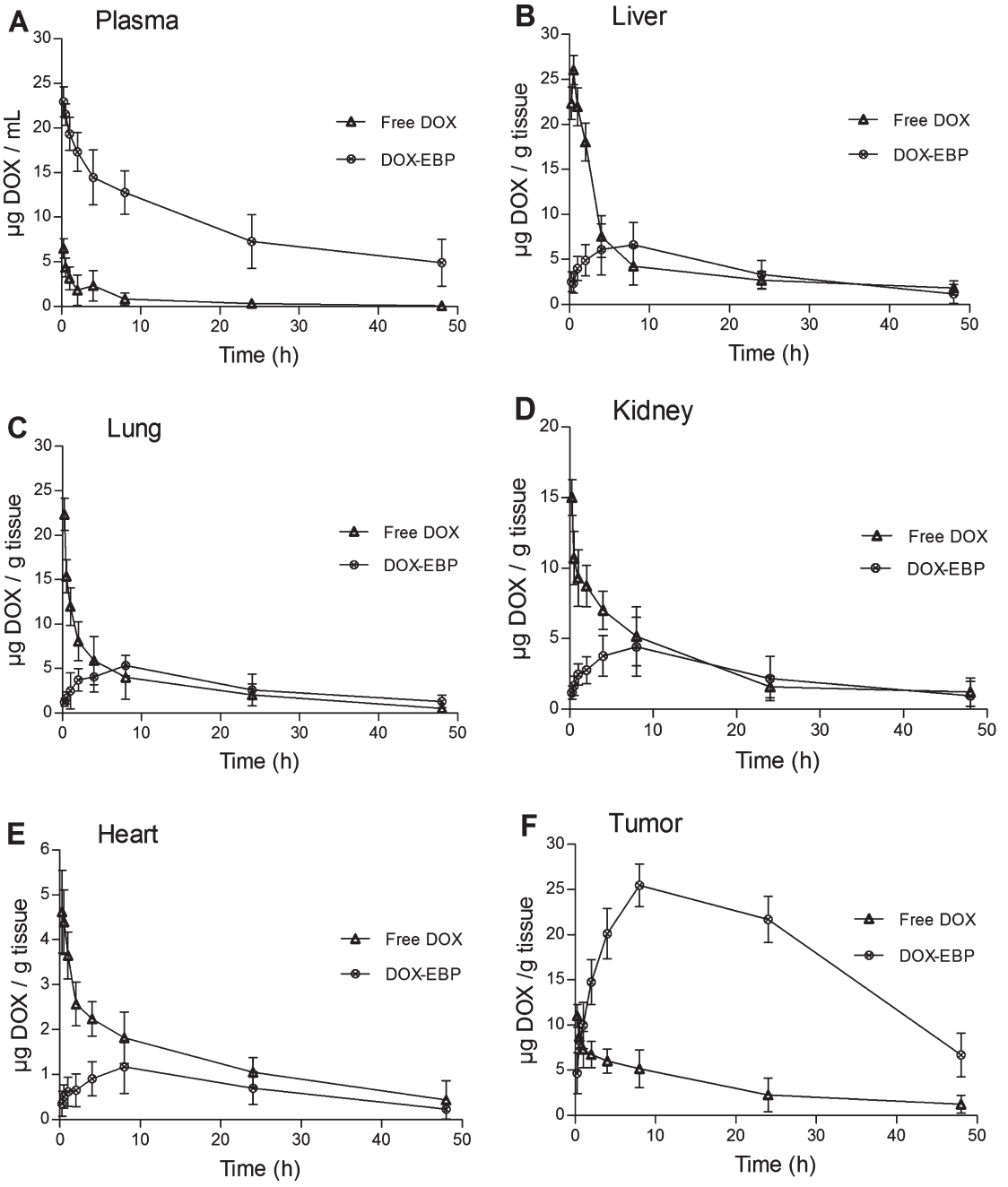

Figure 5. Distribution of free DOX and DOX−EBP conjugate in B16 bearing mice. Murine melanoma B16 cells were injected subcutaneously into C57BL/6 mice, and the tumor was formed in 2 weeks. The animals were then treated with a single dose of free DOX (△) (6 mg/kg) or DOX−EBP (⊗) (6 mg/kg DOX equivalent), and samples from blood and tissues were taken at indicated times. DOX concentration was determined in plasma (A), liver (B), lung (C), kidney (D), heart (E) and tumor tissues (F) by HPLC after drug administration.

Figure 4B). These data suggest that the binding ability of the EBP to EGFR was preserved in the conjugate.

After targeting EGFR-overexpressing cells, the DOX−EBP conjugate may enter tumor cells through EGFR-mediated route. As shown in Figure 2, the competitive anti-EGFR monoclonal antibody C225 can significantly reduce the binding of DOX−EBP conjugate to EGFR, inhibit its entry and result in reduced cellular accumulation of the conjugate in tumor cells. Fluorescent microscopy further shows that the fluorescent signal of DOX−EBP conjugate in both EGFR-overexpressing (SW480) and non-EGFR-overexpressing (MCF-7) cells became very weak after preincubation with C225 (Figure 3C and Figure 4C), demonstrating the inhibition of cellular uptake of the conjugate. These results suggest that the effect of DOX−EBP conjugate was mediated through EGFR.

For a DOX−peptide conjugate to become effective after entering tumor cells, the DOX must be released from the conjugate and enter the nucleus. The availability of active DOX to the nucleus, the drug action site, may become more prominent because the primary mechanism of cytotoxicity of DOX is through intercalation into DNA and disruption of topoisomerase II action.[3] Although DOX can be detected in

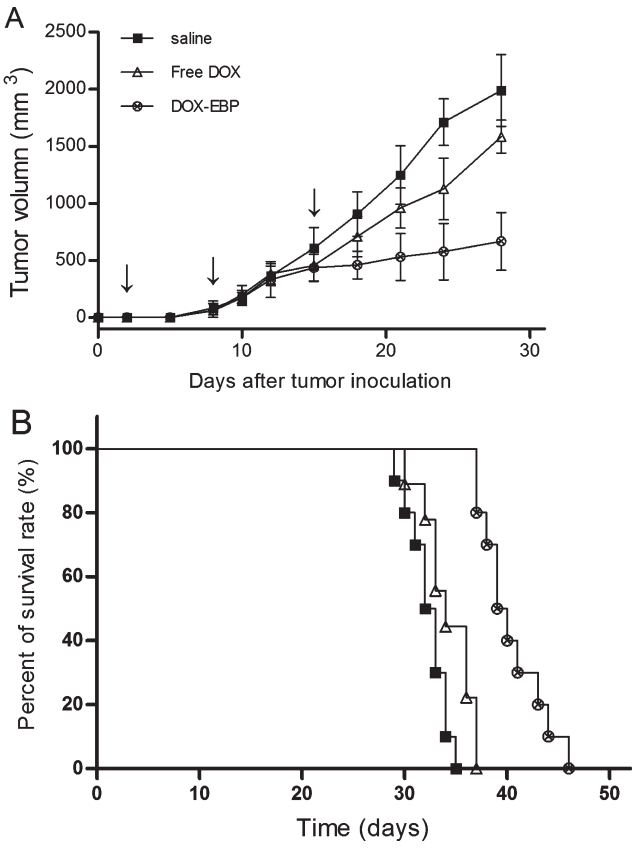

Figure 6. Therapeutic efficacy of free DOX and DOX−EBP in B16 tumor xenograft model. Murine melanoma B16 cells (1×10^7 cells) were injected subcutaneously in C57BL/6 mice. On days 1, 8, and 15 after transplantation of tumors ($n = 9$), free DOX (△) or DOX−EBP (⊗) was injected via tail vein at 5 mg/kg body weight (DOX or DOX equivalent). Control mice received injections of saline (■). (A) Comparison of tumor volume. (B) Survival analysis of B16 tumor-bearing mice (Kaplan−Meier survival curve).

both cytoplasm and nucleus after incubation with free DOX (Figure 3A), the conjugate was clearly distributed in cytoplasm and perinuclear zone, but not in nucleus, after incubation for 30 min (Figure 3B). Similar phenomena were also observed with other peptide carriers conjugated with DOX. For example, the conjugates of a cyclic pentapeptide (CNGRC)[13] and a cell-penetrating peptide (CGGGYGRKKRRQRRR)[50] with DOX exhibited a cytoplasmic distribution, similar to DOX−EBP (Figure 3B). This may be because the large hydrophilic peptides have high hydrogen bonding potential and thus are not readily partitioned into the cell membranes as they are energetically unfavorable to expel hydrogen-bonded water molecules.[51] Therefore, the DOX conjugates inside the cells cannot directly diffuse into the nucleus. On the other hand, during the early incubation period, the active DOX released from the conjugate inside the cytoplasm was not sufficient to be partitioned to the nucleus, therefore its *in vitro* cytotoxicity was not as high as that of free DOX (Table 2). These data demonstrate that the entry and partition routes of the conjugate are distinct from that of free DOX.

Since DOX−EBP conjugate in the current study is an ester conjugate linked via a glutaric acid spacer, it is sensitive to hydrolysis by esterase. Therefore, although the conjugate cannot directly diffuse toward the nucleus, it may be hydrolyzed by cellular esterase to release active DOX in the cytoplasm.[13] As a result, more DOX would be released from the conjugate after extension of time, and penetrate the nuclear envelope and enter the nucleus. As expected, the fluorescent signal of DOX in the nuclei of SW480 cells was stronger after prolonged incubation (24 h) with DOX−EBP (Figure 4B). In contrast, there was no obvious difference between the fluorescent distribution in SW480 cells treated with free DOX for 30 min and 24 h (Figure 3A and 4A). Consequently, the cytotoxic activity of the DOX−EBP conjugate was much higher than that of the original free DOX in SW480 cells after extended incubation (48 h; Table 2).

The binding of DOX−EBP conjugate to EGFR-overexpressing cells suggests that it may have a targeting effect in mice bearing EGFR-overexpressing tumors, therefore we examined the distribution and the antitumor activity of the conjugate *in vivo*. As shown in Figure 5, the administration of DOX−EBP resulted in different biodistribution compared with free DOX. The high content and long circulation time of the conjugate in the bloodstream (Figure 5A) imply the potential of the novel chemotherapeutic agent to achieve a better tumor targeting effect *in vivo*. As shown in Figure 5F, the DOX content was indeed higher in EGFR-overexpressing tumors of B16 cells bearing mice treated with the conjugate than that with free DOX. The substantial delay of the peak concentration of DOX−EBP (at 8 h for DOX−EBP vs 0.5 h for DOX) also suggests that the conjugation of DOX with EBP can enhance its therapeutic efficacy. As expected, after 4 weeks of treatment with DOX−EBP, the tumor volume was reduced 66% compared to the saline control, while the reduction was only 20% when treated with free DOX (Figure 6A). Taken together, these data demonstrate that the DOX−EBP conjugate had exhibited longer circulation time and greater accumulation in EGFR over-expressing tumors, and thus lead to increased therapeutic efficacy. Similar results have also been reported for DOX conjugated with other peptides.[52,53]

The adverse effect is a major concern for free DOX as a therapeutic agent, and the nonselective toxicity of DOX is closely related to its distribution in normal tissues at high levels. The DOX−EBP conjugate, however, effectively lowered the distribution of DOX in normal tissues, in particular with no significant accumulation in the heart tissue, which is extremely sensitive to DOX toxicity (Figure 5B−E). Furthermore, treatment with DOX−EBP conjugate significantly extended the survival time of mice bearing tumor xenograft (Figure 6B), demonstrating lower systemic toxicity and higher therapeutic efficacy.

In conclusion, we report the conjugation of DOX with an EGFR-binding peptide (EBP: NH_2-CMYIEALDKYAC-COOH) via an ester bond at C_{14} through a glutarate spacer, and demonstrate that the DOX−EBP conjugate efficiently retained the EGFR binding ability. The conjugate displayed targeting competence toward EGFR-overexpressing tumor cells, and thus exhibited potent antitumor effect *in vivo*.

AUTHOR INFORMATION

Corresponding Author

*S.A. and Z.H.: College of Pharmacy, Wuhan University, 185 East Lake Road, Wuhan 430071, China. Phone: 86-27-68759006. Fax: 86-27-68759850. E-mail: aishibin@tom.com (S.A.); zbhuang@whu.edu.cn (Z.H.).

ACKNOWLEDGMENT

This study was supported by the National Mega Project on Major Drug Development (Grant No. 2009ZX09301-014-1),

the National Natural Science Foundation of China (Grant No. 30971456) and in part by the National High-Tech R & D Program of China (863 Program; Grant No. 2007AA10Z344).

REFERENCES

(1) Gewirtz, D. A. A critical evaluation of the mechanisms of action proposed for the antitumor effects of the anthracycline antibiotics adriamycin and daunorubicin. *Biochem. Pharmacol.* **1999**, *57*, 727–741.

(2) Lal, S.; Mahajan, A.; Chen, W. N.; Chowbay, B. Pharmacogenetics of target genes across doxorubicin disposition pathway: a review. *Curr. Drug Metab.* **2010**, *11*, 115–128.

(3) Minotti, G.; Menna, P.; Salvatorelli, E.; Cairo, G.; Gianni, L. Anthracyclines: molecular advances and pharmacologic developments in antitumor activity and cardiotoxicity. *Pharmacol. Rev.* **2004**, *56*, 185–229.

(4) Thornton, K. Chemotherapeutic management of soft tissue sarcoma. *Surg. Clin. North Am.* **2008**, *88*, 647–660.

(5) Raschi, E.; Vasina, V.; Ursino, M. G.; Boriani, G.; Martoni, A.; De Ponti, F. Anticancer drugs and cardiotoxiciy: Insights and perspectives in the era of targeted therapy. *Pharmacol. Ther.* **2010**, *125*, 196–218.

(6) Mordente, A.; Meucci, E.; Silvestrini, A.; Martorana, G. E.; Giardina, B. New developments in anthracycline-induced cardiotoxicity. *Curr. Med. Chem.* **2009**, *16*, 1656–1672.

(7) Ferreira, A. L.; Matsubara, L. S.; Matsubara, B. B. Anthracycline-induced cardiotoxicity. *Cardiovasc. Hematol. Agents Med. Chem.* **2008**, *6*, 278–281.

(8) Langer, M.; Kratz, F.; Rothen-Rutishauser, B.; Wunderli-Allenspach, H.; Beck-Sickinger, A. G. Novel peptide conjugates for tumor-specific chemotherapy. *J. Med. Chem.* **2001**, *44*, 1341–1348.

(9) Nagy, A.; Schally, A. V. Targeting of cytotoxic luteinizing hormone-releasing hormone analogs to breast, ovarian, endometrial, and prostate cancer. *Biol. Reprod.* **2005**, *73*, 851–859.

(10) de Groot, F. M.; Broxterman, H. J.; Adams, H. P.; van Vliet, A.; Tesser, G. I.; Elderkamp, Y. W.; Schraa, A. J.; Kok, R. J.; Molema, G.; Pinedo, H. M.; Scheeren, H. W. Design, synthesis, and biological evaluation of a dual tumor-specific motive containing integrin-targeted plasmin-cleavable doxorubicin prodrug. *Mol. Cancer Ther.* **2002**, *1*, 901–911.

(11) Qian, Z. M.; Li, H.; Sun, H.; Ho, K. Targeted drug delivery via the transferrin receptor-mediated endocytosis pathway. *Pharmacol. Rev.* **2002**, *54*, 561–587.

(12) Schally, A. V.; Nagy, A. New approaches to treatment of various cancers based on cytotoxic analogs of LHRH, somatostatin and bombesin. *Life Sci.* **2003**, *72*, 2305–2320.

(13) van Hensbergen, Y.; Broxterman, H. J.; Elderkamp, Y. W.; Lankelma, J.; Beers, J. C.; Heijn, M.; Boven, E.; Hoekman, K.; Pinedo, H. M. A doxorubicin-CNGRC conjugate with prodrug properties. *Biochem. Pharmacol.* **2002**, *63*, 897–908.

(14) Emons, G.; Sindermann, H.; Engel, J.; Schally, A. V.; Gründker, C. Luteinizing hormone-releasing hormone receptor-targeted chemotherapy using AN-152. *Neuroendocrinology* **2009**, *90*, 15–18.

(15) Dutta, P. R.; Maity, A. Cellular responses to EGFR inhibitors and their relevance to cancer therapy. *Cancer Lett.* **2007**, *254*, 165–177.

(16) Herbst, R. S. Review of epidermal growth factor receptor biology. *Int. J. Radiat. Oncol. Biol. Phys.* **2004**, *59*, 21–26.

(17) Harari, P. M.; Allen, G. W.; Bonner, J. A. Biology of interactions: antiepidermal growth factor receptor agents. *J. Clin. Oncol.* **2007**, *25*, 4057–4065.

(18) Okamoto, I. Epidermal growth factor receptor in relation to tumor development: EGFR-targeted anticancer therapy. *FEBS. J.* **2010**, *277*, 309–315.

(19) Schneider, M. R.; Wolf, E. The epidermal growth factor receptor ligands at a glance. *J. Cell Physiol.* **2009**, *218*, 460–466.

(20) Cooke, R. M.; Wilkinson, A. J.; Baron, M.; Pastore, A.; Tappin, M. J.; Campbell, I. D.; Gregory, H.; Sheard, B. The solution structure of human epidermal growth factor. *Nature* **1987**, *327*, 339–341.

(21) Montelione, G. T.; Wüthrich, K.; Nice, E. C.; Burgess, A. W.; Scheraga, H. A. Solution structure of murine epidermal growth factor: determination of the polypeptide backbone chain-fold by nuclear magnetic resonance and distance geometry. *Proc. Natl. Acad. Sci. U.S.A.* **1987**, *84*, 5226–5230.

(22) Koide, H.; Muto, Y.; Kasai, H.; Kohri, K.; Hoshi, K.; Takahashi, S.; Tsukumo, K.; Sasaki, T.; Oka, T.; Miyake, T. A site-directed mutagenesis study on the role of isoleucine-23 of human epidermal growth factor in the receptor binding. *Biochim. Biophys. Acta* **1992**, *1120*, 257–261.

(23) Wingens, M.; Walma, T.; van Ingen, H.; Stortelers, C.; van Leeuwen, J. E.; van Zoelen, E. J.; Vuister, G. W. Structural analysis of an epidermal growth factor/transforming growth factor-alpha chimera with unique ErbB binding specificity. *J. Biol. Chem.* **2003**, *278*, 39114–39123.

(24) Ogiso, H.; Ishitani, R.; Nureki, O.; Fukai, S.; Yamanaka, M.; Kim, J. H.; Saito, K.; Sakamoto, A.; Inoue, M.; Shirouzu, M.; Yokoyama, S. Crystal structure of the complex of human epidermal growth factor and receptor extracellular domains. *Cell* **2002**, *110*, 775–787.

(25) Komoriya, A.; Hortsch, M.; Meyers, C.; Smith, M.; Kanety, H.; Schlessinger, J. Biologically active synthetic fragments of epidermal growth factor: localization of a major receptor-binding region. *Proc. Natl. Acad. Sci. U.S.A.* **1984**, *81*, 1351–1355.

(26) Wilson, C. L.; Monteith, W. B.; Danell, A. S.; Burns, C. S. Purification and characterization of the central segment of prothymosin-alpha: methodology for handling highly acidic peptides. *J. Pept. Sci.* **2006**, *12*, 721–725.

(27) Nagy, A.; Schally, A. V.; Armatis, P.; Szepeshazi, K.; Halmos, G.; Kovacs, M.; Zarandi, M.; Groot, K.; Miyazaki, M.; Jungwirth, A.; Horvath, J. Cytotoxic analogs of luteinizing hormone-releasing hormone containing doxorubicin or 2-pyrrolinodoxorubicin, a derivative 500−1000 times more potent. *Proc. Natl. Acad. Sci. U.S.A.* **1996**, *93*, 7269–7273.

(28) Chen, Q.; Sowa, D. A.; Gabathuler, R. Synthesis of doxorubicin conjugates through 14-hydroxy group to melanotransferrin P97. *Synth. Commun.* **2003**, *33*, 2389–2398.

(29) Bai, L.; Zhu, R.; Chen, Z.; Gao, L.; Zhang, X.; Wang, X.; Bai, C. Potential role of short hairpin RNA targeting epidermal growth factor receptor in growth and sensitivity to drugs of human lung adenocarcinoma cells. *Biochem. Pharmacol.* **2006**, *71*, 1265–1271.

(30) Bidwell, G. L., 3rd.; Davis, A. N.; Fokt, I.; Priebe, W.; Raucher, D. A thermally targeted elastin-like polypeptide-doxorubicin conjugate overcomes drug resistance. *Invest. New Drugs* **2007**, *25*, 313–326.

(31) Overholser, J. P.; Prewett, M. C.; Hooper, A. T.; Waksal, H. W.; Hicklin, D. J. Epidermal growth factor receptor blockade by antibody IMC-C225 inhibits growth of a human pancreatic carcinoma xenograft in nude mice. *Cancer* **2000**, *89*, 74–82.

(32) Abbosh, P. H.; Montgomery, J. S.; Starkey, J. A.; Novotny, M.; Zuhowski, E. G.; Egorin, M. J.; Moseman, A. P.; Golas, A.; Brannon, K. M.; Balch, C.; Huang, T. H.; Nephew, K. P. Dominant-negative histone H3 lysine 27 mutant derepresses silenced tumor suppressor genes and reverses the drug-resistant phenotype in cancer cells. *Cancer Res.* **2006**, *66*, 5582–5591.

(33) Pang, Z.; Feng, L.; Hua, R.; Chen, J.; Gao, H.; Pan, S.; Jiang, X.; Zhang, P. Lactoferrin-conjugated biodegradable polymersome holding doxorubicin and tetrandrine for chemotherapy of glioma rats. *Mol. Pharmaceutics* **2010**, *7*, 1995–2005.

(34) Cao, N.; Feng, S. S. Doxorubicin conjugated to D-alpha-tocopheryl polyethylene glycol 1000 succinate (TPGS): conjugation chemistry, characterization, in vitro and in vivo evaluation. *Biomaterials* **2008**, *29*, 3856–3865.

(35) Mosmann, T. Rapid colorimetric assay for cellular growth and survival: application to proliferation and cytotoxicity assays. *J. Immunol. Methods* **1983**, *65*, 55–63.

(36) Han, L.; Wang, W.; Fang, Y.; Feng, Z.; Liao, S.; Li, W.; Li, Y.; Li, C.; Maitituoheti, M.; Dong, H.; Lai, W.; Gao, Q.; Xi, L.; Wu, M.; Wang, D.; Zhou, J.; Meng, L.; Wang, S.; Ma, D. Soluble B and T lymphocyte attenuator possesses antitumor effects and facilitates heat shock protein 70 vaccine-triggered antitumor immunity against a murine TC-1 cervical cancer model *in vivo*. *J. Immunol.* **2009**, *183*, 7842–7850.

(37) Mamot, C.; Drummond, D. C.; Noble, C. O.; Kallab, V.; Guo, Z.; Hong, K.; Kirpotin, D. B.; Park, J. W. Epidermal growth factor receptor−targeted immunoliposomes significantly enhance the efficacy of multiple anticancer drugs *in vivo*. *Cancer Res.* **2005**, *65*, 11631–11638.

(38) Etrych, T.; Chytil, P.; Mrkvan, T.; Sírová, M.; Ríhová, B.; Ulbrich, K. Conjugates of doxorubicin with graft HPMA copolymers for passive tumor targeting. *J. Controlled Release* **2008**, *132*, 184–192.

(39) Al-Abd, A. M.; Kim, N. H.; Song, S. C.; Lee, S. J.; Kuh, H. J. A simple HPLC method for doxorubicin in plasma and tissues of nude mice. *Arch. Pharm. Res.* **2009**, *32*, 605–611.

(40) Wu, G.; Barth, R. F.; Yang, W.; Kawabata, S.; Zhang, L.; Green-Church, K. Targeted delivery of methotrexate to epidermal growth factor receptor-positive brain tumors by means of cetuximab (IMC-C225) dendrimer bioconjugates. *Mol. Cancer Ther.* **2006**, *5*, 52–59.

(41) Goldstein, N. I.; Prewett, M.; Zuklys, K.; Rockwell, P.; Mendelsohn, J. Biological efficacy of a chimeric antibody to the epidermal growth factor receptor in a human tumor xenograft model. *Clin. Cancer Res.* **1995**, *1*, 1311–1318.

(42) Pohl, M.; Stricker, I.; Schoeneck, A.; Schulmann, K.; Klein-Scory, S.; Schwarte-Waldhoff, V.; Hasmann, M.; Tannapfel, A.; Schmiegel, W.; Reinacher-Schick, A. Antitumor activity of the HER2 dimerization inhibitor pertuzumab on human colon cancer cells in vitro and in vivo. *J. Cancer Res. Clin. Oncol.* **2009**, *135*, 1377–1386.

(43) Liao, X.; Che, X.; Zhao, W.; Zhang, D.; Long, H.; Prakash, C.; Li, H. Effects of propranolol in combination with radiation on apoptosis and survival of gastric cancer cells in vitro. *Radiat. Oncol.* **2010**, *5*, 58.

(44) Ueno, Y.; Sakurai, H.; Tsunoda, S.; Choo, M. K.; Matsuo, M.; Koizumi, K.; Saiki, I. Heregulin-induced activation of ErbB3 by EGFR tyrosine kinase activity promotes tumor growth and metastasis in melanoma cells. *Int. J. Cancer* **2008**, *123*, 340–347.

(45) Hirsch, D. S.; Shen, Y.; Wu, W. J. Growth and motility inhibition of breast cancer cells by epidermal growth factor receptor degradation is correlated with inactivation of Cdc42. *Cancer Res.* **2006**, *66*, 3523–3523.

(46) Lurje, G.; Lenz, H. J. EGFR signaling and drug discovery. *Oncology* **2009**, *77*, 400–410.

(47) Mitsudomi, T.; Yatabe, Y. Epidermal growth factor receptor in relation to tumor development: EGFR gene and cancer. *FEBS. J.* **2010**, *277*, 301–308.

(48) Meyer-Losic, F.; Quinonero, J.; Dubois, V.; Alluis, B.; Dechambre, M.; Michel, M.; Cailler, F.; Fernandez, A. M.; Trouet, A.; Kearsey, J. Improved therapeutic efficacy of doxorubicin through conjugation with a novel peptide drug delivery technology (Vectocell). *J. Med. Chem.* **2006**, *49*, 6908–6916.

(49) Halmos, G.; Nagy, A.; Lamharzi, N.; Schally, A. V. Cytotoxic analogs of luteinizing hormone-releasing hormone bind with high affinity to human breast cancers. *Cancer Lett.* **1999**, *136*, 129–136.

(50) Liang, J. F.; Yang, V. C. Synthesis of doxorubicin-peptide conjugate with multidrug resistant tumor cell killing activity. *Bioorg. Med. Chem. Lett.* **2005**, *15*, 5071–5075.

(51) Lipinski, C. A.; Lombardo, F.; Dominy, B. W.; Feeney, P. J. Experimental and computational approaches to estimate solubility and permeability in drug discovery and development settings. *Adv. Drug Delivery Rev.* **2001**, *46*, 3–26.

(52) Szepeshazi, K.; Schally, A. V.; Halmos, G. LH-RH receptors in human colorectal cancers: unexpected molecular targets for experimental therapy. *Int. J. Oncol.* **2007**, *30*, 1485–1492.

(53) Wu, W.; Luo, Y.; Sun, C.; Liu, Y.; Kuo, P.; Varga, J.; Xiang, R.; Reisfeld, R.; Janda, K. D.; Edgington, T. S.; Liu, C. Targeting cell-impermeable prodrug activation to tumor microenvironment eradicates multiple drug-resistant neoplasms. *Cancer Res.* **2006**, *66*, 970–980.